Wave front engineering for microscopy of living cells.

Valentina Emiliani, Dan Cojoc, Enrico Ferrari, Valeria Garbin, Christiane Durieux, Maite Coppey-Moisan, Enzo Di Fabrizio

Wave front engineering for microscopy of living cells with simultaneous optical sectioning and multi trap optical tweezers

Valentina Emiliani,[1] Dan Cojoc,[2] Enrico Ferrari,[2] Valeria Garbin,[2]
Christiane Durieux,[1] Maite Coppey-Moisan,[1] and Enzo Di Fabrizio[2]

[1]*Institut Jacques Monod, UMR 7592, CNRS,*
Universités P6/P7, 75251 Paris cedex 05, France
[2]*INFM-TASC (Istituto Nazionale per la Fisica della Materia,*
laboratorio nazionale Tecnologie Avanzate e nanoSCienze),
LILIT Beamline, at Elettra Sincrotrone,
S.S.14 Km 163.5, I-34012, Basovizza (Trieste), Italy

(Dated: January 5, 2005)

Abstract

A new method to perform simultaneously three dimensional optical sectioning and optical manipulation is presented. The system combines a multi trap optical tweezers with a video microscope to enable axial scanning of living cells while maintaining the trapping configuration at a fixed position. To compensate the axial movement of the objective, a home made software addresses a spatial light modulator which modifies the wave front of the trapping laser beam. This method has been validated in three different experimental configurations. In the first, we decouple the position of a trapping plane from the axial movements of the objective and perform optical sectioning of a circle of beads kept on a fixed plane. In a second experiment, we extend the method to living cell microscopy by showing that mechanical constraints can be applied on the dorsal surface of a cell whilst performing its fluorescence optical sectioning. Finally, we trapped beads in a three dimensional geometry and perform, always through the same objective, an axial scan of the volume delimited by the beads.

INTRODUCTION

In recent years, the advance in imaging methods has become apparent in biology, due to the tremendous progress in fluorescence tagging techniques and nano-metric probes. Nowadays, high-spatial and temporal resolution techniques as confocal [1], two-photon [2] total internal reflection microscopy (TIRF) [3] or fluorescence lifetime imaging microscopy [4, 5] permit to look at subcellular details and macromolecular organization with sub-micrometer resolution.

The possibility to optically explore the complex mechanisms which regulate cell function in living cells on a nanoscopic scale has generated, in parallel, the need for the development of manipulation techniques with a comparable resolution.

Optical tweezers (OT) enable an all-optical manipulation of matter with micrometer precision, piconewton control of the applied forces and, at present, is one of the most promising manipulation technique operating with minimal invasion in biology [6]. It permits manipulation of micrometric and submicrometric biological samples as viruses, bacteria, DNA and living cells [7–10]. The movement and force of motor proteins can be measured by attaching micron-sized beads to single motor proteins [11, 12]. Cellular force transduction [13–17] or membrane elasticity [18] can be measured by inducing controlled localized forces or tensions via the attachment of beads on cell membranes.

The successive introduction of multi trap [19] optical tweezers has extended these manipulations to different objects simultaneously and recently it has been used to demonstrate multi force optical tweezers [20] where the force of each trap can be adjusted individually .

Furthermore, the recent advent of spatial light modulators, has permitted to evolve from the 'conventional' optical tweezers systems towards the so called dynamical holographic optical tweezers. Here, thanks to the *wave-front engineering* of the trapping beam, it is possible to generate multiple traps in three dimensional (3D) geometries and to dynamically reconfigure them [21–24]. Moreover the intensity profile of each spot can individually be modified allowing for complex arrangement of traps based on different modes. For example, the trapping beam can be shaped to generate optical vortices [25, 26] which carry orbital angular momentum that can be transferred to the trapped objects. Optical vortices have been demonstrated to be useful to trap reflecting-, absorbing- or low-index- particles and to rotate microscopic objects thus opening new prospectives otherwise not possible with a

conventional OT system.

A further advance in the development of optical techniques for biological research is represented now by the combination of the progresses made in high temporal-and spatial-resolution imaging with those attained in optical manipulation.

Up to date, in most of the OT microscopes a wide field epi-fluorescence scheme is used. Very recently, to improve the optical resolution, new imaging solutions start to be exploited as presented in Ref. [27]. In this paper the authors measured the mechanical transitions corresponding to single DNA hybrid ruptures by combining TIRF and OT. They simultaneously achieved, in the near-field volume, pN force measurements and single molecule fluorescence detection.

To further exploit the potentiality of an OT system with a high resolution imaging set up, a possibility is to incorporate into the OT microscope a 3D scanning optical technique. However, this combination presents technical challenges when the trapping and imaging beams are combined by the same objective lens. One problem encountered in this configuration is that the axial movement of the microscope objective inevitably displaces the trapping plane of the same amount.

Alternatively, two objective lenses head-on with completely dissociated beam steering optics can be used. This configuration is however incompatible with the possibility to perform differential interference contrast (DIC). Moreover, to optimize both the quality of the optical traps and the optical resolution of the imaging system, oil or water immersion objectives with a high numerical aperture (≥ 1.2) and therefore a short working distance are largely preferred. Therefore, this configuration limits the sample thickness and the possibility to mount on the upper part of the microscope additional tools as micromanipulators or microinjectors, and definitively hamper an easy switch from fluorescence to transmission measurements.

Very recently, M. Goksör and colleagues [28] have combined a trapping- and a multiphoton-beam using a single objective. An external lens has been translated to control the divergence of the trapping laser and optical sectioning has been achieved by moving the trapped object through the image plane. However, this solution is inappropriate for imaging planes axially distinguished from the trapping plane.

One solution to this problem has been presented in Ref. [29], where a confocal and an OT microscope have been combined by coupling the trapping beam into an optical fiber mounted

on a translation stage. In this way, the objective displacements have been compensated with a synchronized reverse motion of the trapping plane. However, the system is limited to a single optical trap.

To overcome these limits, in this paper we present an alternative method which consists in shaping the trapping beam via digital addressing a Liquid Crystal Spatial Light Modulator (LC-SLM). The wave front of the trapping beam is modified to compensate the movement of the objective by projecting on the LC-SLM fast moving correctional diffractive optical elements (DOEs). As a result, we can keep the optical traps at a fixed position whilst the objective is moved. The advantage of the proposed technique is that we can fully exploit the benefits of using a holographic optical tweezers system, such as the possibility to generate and move multiple traps, eventually organized in 3D geometries and/or in different modes, in combination with those of a 3D optical scanning technique.

The capability of our system is demonstrated in three different experiments. In a first one, we show that we can decouple the position of a trapping plane from the axial movements of the objective by performing optical sectioning of a circle of trapped beads. In a second experiment, we use a similar scheme to apply mechanical constraints on the dorsal surface of a cell whilst performing 3D optical sectioning of the cell. To this end, the nucleus of HeLa cells have been fluorescently labeled with H2B-GFP and a circular array of micro beads is attached on the dorsal surface of the cell and kept at a fixed position during the fluorescence and transmission sectioning. Finally, we extend our method to a 3D beads volume. Silica beads are organized in a 3D geometry and we show that we can simultaneously control the position of different planes while performing axial optical sectioning.

RESULTS

Microscope design

The microscope is based on a standard inverted microscope (Zeiss AxioVert 135) with differential interference contrast (DIC), and epi-fluorescence. The attenuated and expanded (3X) 1064-nm beam of a 10W single-mode CW fiber laser (IPG Photonics YLM-10) is directed onto the LC-SLM, reflected into the side port of the microscope and directed with an IR dichroic mirror to the focusing objective (100x NA-1.3 oil). To allow simultaneous

recording of fluorescence and DIC while using the optical traps, the dichroic is positioned above the fluorescence filter block. In this way, the excitation light from a Mercury lamp mounted on the rear port of the microscope is focused into the sample by the same objective used for trapping. Fluorescence from the sample is sent to a high sensitive CCD camera (Cool Snap HQ, Roper) placed at the exit port of the microscope. To obtain DIC images, a polarizer is inserted below the fluorescence block filter and crossed with the DIC analyzer positioned above the microscope condenser.

In order to perform 3D optical sectioning, the objective is mounted on a nanofocusing positioner (PI Instruments, *PIFOC* 721.10). To improve the resolution, the collected images are de-convoluted afterward by the programm Huygens (Scientific Volume Imaging), with the algorithm QMLE and using experimental Point Spread Functions (PSF) of 0.17 μm fluorescent beads (Molecular Probe).

The SLM (Hamamatsu PPM-X8267) is a programable phase modulator that uses an optical image transmitting element to couple an optically-addressed Parallel Aligned Nematic Liquid Crystal SLM (PAL-SLM) with an electrically-addressed intensity modulator.

A spherical wave approach [24, 30] is used to calculate phase DOEs which are displayed on the SLM to transform the incoming laser beam into a distribution of laser spots, each with individually specified characteristics and arranged in an arbitrary desired geometrical configurations.

A schematic of the optical set up is presented in Figure 1(a). The trapping beam path (red lines) comprises the laser source (L), the SLM, the dichroic mirror (DM) and the microscope objective (MO). The distance between the SLM and the MO first principal plane is d. f_{SLM} and f_{MO} are the focal lengths of the DOE implemented on the SLM and of the objective, respectively. Finally, z indicates the axial position of the trapping plane with respect to the objective focal plane, F_{MO}, and depends on the value of f_{SLM} that we set for the DOE. From the scheme in Figure 1 (a), as explained in Methods, we can derive a simple formula which relates the focal length, f_{SLM} to the axial trapping position z:

$$f_{SLM} = d - f_{MO} - \frac{f_{MO}^2}{z}, \tag{1}$$

Once the two fixed parameters d and f_{MO} are known, Equation 1 permits to derive for each position of the trapping plane, z, the focal length, f_{SLM}. As explained in Methods, we derived the values for d, and f_{MO} by fitting the calibration curve shown in Figure 1(b).

The generation and manipulation of spots in 3D volumes may require to collect images from optical planes different from the objective's focal plane. Therefore we have modified the optical path from the sample to the imaging camera (green lines) by adding a 1:1 telescope (T) in front of the CCD, as shown in Figure 1(a). The telescope, T, and the CCD are mounted on a translation stage that allows us to adjust the position z_1 of the imaging plane by a rigid translation, D, of the telescope T and the CCD (see Methods).

The efficacy of this imaging approach is demonstrated in Figure 1(c). Here 7 silica beads are trapped in 3 different planes separated along the axial direction by a distance of 2μm. The intermediate plane is at 9.6 μm from the objective focal plane. The diameters of the bottom and intermediate planes are 14μm and 10.5μm, respectively. The image shown in Figure 1(c) has been acquired by adjusting the position of (T+CCD) in order to have the imaging plane coincident with the intermediate plane of the structure, i.e. at z_1=9.6μm, the bottom and top plane are out of focus but still visible.

3D Optical sectioning and multi trap optical tweezers

In this section, we first present an experiment where we decouple the position of a 2D trapping plane from the axial movement of the microscope objective. In a second experiment we apply a similar scheme to perform optical sectioning of a fluorescently labeled living cell while keeping a circular array of micro beads attached on its dorsal surface. Finally, we extend the method to perform an axial scanning of a 3D volume of beads.

The use of a DOE gives rise to a non diffracted order which is focused on the focal plane of the microscope objective: the zero order spot. The latter can induce cell damaging and generate an extra signal that adds up to the fluorescence signal. In the following experiments, this two undesired effects are avoided by generating laser traps far enough from the objective focal plane and choosing the observation volumes out of this plane.

For the first experiment, we have calculated a temporal sequence of 46 phase DOEs that produce a circular array of 6 laser traps (diameter of 10μm) and keep it at a fixed position in respect to the coverslip while moving the objective over a distance of 9.2 μm by steps of 200 nm. Silica beads (2.34μm in diameter) diluted in water are trapped in the generated spots. DIC images are acquired at each step of the optical sectioning.

As schematized in Figure 2, there are three optical planes to be considered:

(i) *the objective focal plane* (in gray) which coincides with the focusing plane for the zero order spot: this plane is at fixed distance, f_{MO}, from the principal plane of the objective, while it position, z_{ob}, with respect to the coverslip is varied during the axial scan.

(ii) *the imaging plane* (in green): in a conventional microscope it would coincide with the objective focal plane, here it can be adjusted to an arbitrary axial plane by regulating the imaging path, (T+CCD). During the scan this plane lies at a fixed position, z_1, from the objective focal plane and at a variable position, z_{IP}, from the coverslip. For the first experiment we set z_1=9.6 μm.

(iii) *the trapping plane* (in red): its position, z, relative to the objective focal plane, depends on the focal length, f_{SLM}, that we set for the DOE (Equation 1). During the optical sectioning, the values of f_{SLM} are varied in such a way that the trapping plane is kept *at a constant position, z_0, from the coverslip.*

Figures. 3(a)-(f) show six cross sections from the optical sectioning of the circle of beads. In the same field, part of a pattern on the coverslip is visible. From the left to the right the objective moves down to the coverslip, as demonstrated by the pattern which is gradually coming into focus. Correspondingly, the imaging plane moves from z_{IP}^{in}= +9.2 μm to z_{IP}^{fin}= 0 μm. To compensate the objective movements, the distance z between the trapping and the objective focal plane is varied between z^{in}= +5 μm to z^{fin}= +14.2 μm. As a results, the circle of beads is kept at a constant hight, z_0=4.6 μm, during the whole scan. This is evident by looking at the sequence of images (Figures. 3(a)-(f)) which shows the circle of beads out of focus at the beginning and at the end of the axial scan and in focus at the half of the scan.

In a second experiment we demonstrated the potentiality of the compensation method in living cell microscopy. Similar to the previous experiment, a sequence of phase DOEs which generates a circular array of 6 beads disposed on a circle of 15μm diameter is addressed onto the SLM. Silica beads are trapped onto the circle and held on the dorsal surface of a living HeLa cell. The mechanical interaction between cell cytoskeleton and beads is induced by coating the beads with arginine-glycine-aspartic acid (RGD). A small peptide contained in the tenth type III domain of the fibronectine which plays a central role in cell adhesion [31].

The cell is transfected with H2B-GFP, which enables to observe the cell nucleus by recording the GFP fluorescence.

Wide field optical sectioning of the cell is performed by moving the objective and therefore

the imaging plane from z_{IP}^{in}= +12.6 μm to z_{IP}^{fin}= 4.4 μm. At the same time the trapping plane for the beads is kept at z_0=8μm by running the sequence of DOEs that compensate for the objective movement (z^{in}= +5 μm to z^{fin}= +13.2 μm). At each position of the objective, we acquired a transmission and a fluorescence image. To improve the resolution of the 3D scan, the fluorescence images have been afterward de-convoluted by the Huygens program. The experimental PSF for the de-convolution has been measured in the same imaging condition. A sequence of transmission and fluorescence images acquired during the optical sectioning of an HeLa cell are shown in Figure 4 (a) and (b). For $z_{IP} \simeq +8\mu$m the imaging plane overlaps with the trapping plane as is reveled by the transmission sequence (Figure 4 (a)). The cell nucleus is crossed by the imaging plane towards the end of the scan, as it appear from the fluorescence sequence shown in Figure 4 (b).

Finally, we performed an optical sectioning of beads trapped in the 3D geometry of Figure 1(c). In this case, we wanted to keep constant during the axial scan the position *and* the 3D shape of the structure. Therefore the movement of the objective has been compensated by calculating, for each step, the DOEs necessary to simultaneously move backwards the three planes of the 3D array of beads. Figure 5(a)-(f) shows a selected sequence of images taken during an axial scan performed from z_{IP}^{in}= +12.6 μm to z_{IP}^{fin}= 7.4 μm with a step of 200 nm. The three planes of the structure are coming in to focus each time that the imaging plane coincides with one of them (Figures 5(a),(e),(f)).

DISCUSSION

We have presented a new method for biological microscopy which enables to perform simultaneously 3D optical manipulation and optical sectioning. This technique enables to decouple the imaging and the trapping planes using the same objective. We change the imaging plane position via a mechanical movement of the objective while the position of the trapping beam is modified by engineering its wave front through a digitally addressed LC-SLM. The DOEs profiles that we used to address the LC-SLM are calculated by using a home made software based on a spherical wave approach. Moreover we have presented a modification of the microscope imaging path which allows us to image planes distinguished from the objective focal plane. Interestingly, our method can be easily extended to the case where optical manipulation is performed in combination with other optical scanning

techniques as confocal or two photon microscopy.

To illustrate the potentiality of our method, we have performed three experiments. In the first, we have shown that we can move the imaging plane in respect to the trapping plane by performing a 3D optical sectioning of a circle of micrometric beads kept by the laser. This approach is very useful for high resolution optical sectioning of motile biological samples such as bacteria, non adherent cells, spermatozoa etc. In this case one can hold the sample with the trapping beam and simultaneously perform the 3D optical sectioning of the trapped object. Moreover, the possibility to generate multi traps allows one to manipulate many samples at the same time and to control their relative position. Consequently one can use this manipulation to study the mutual spatial influence between interacting cells during their optical sectioning. Finally, by modifying the mode of the optical traps one can imagine to extend this technique for optical sectioning of absorbing-, reflecting- or low index-samples.

In the last decade, several experiments have shown that cells can sense mechanical forces coming from their environment. Such mechanotransduction occurs primarily at adhesive contacts where membrane receptors make a physical-chemical link between the extracellular matrix and the cytoskeleton. To dissect these processes, a typical experiment consists in using OT to place microspheres coated with specific extracellular ligands on the dorsal surface of cells and probe the resistance of the receptor-cytoskeleton connection e.g by monitoring the recruitment or activation of specific proteins. [13–17] In the second experiment of this paper, we have shown that we can control the position of a circle of beads on a cell cortex whilst performing optical sectioning through the cell. We can therefore add to previous experimental schemes the possibility to monitor cell reaction to external mechanical constrains on planes different from the plane where the constraints are applied. Consequently one can reconstruct 3D map of cellular mechanotransduction and follow how the effects of mechanical constraints propagate in the cell.

Finally, in the last experiment we have shown that we can control and fix the position of optical traps located on different axial planes while simultaneously performing a 3D optical sectioning of the volume delimited by the planes. With this experimental scheme we can imagine to extend the previous experiment to the case where mechanical constraints are distributed in 3D patterns. As already shown, the rapid refreshing rate of the SLM enables to dynamically adapt the distribution of the optical traps to the cell shape and

to hold a 3D volumes of beads on cell cortexes [32]. The combination of a holographic microscope and a 3D optical sectioning technique will allows us to complete this kind of manipulation with the possibility to monitor the effect of a 3D pattern of forces on cellular force mechanotransduction.

As a final remark, we note that a similar approach is not limited to decouple an imaging and a trapping beam, but one can imagine to extend the same method to decouple an imaging path from any *perturbation beam* e.g a photoactivating-, uncaging- or scissor-laser.

METHODS

Imaging path

In the presented microscope, it is crucial to have the possibility to focus objects located on plane axially distinguished from the objective's focal plane. To this end, the microscope needed an adaptation of the optical path from the sample to the imaging CCD, as is schematized in Figure 1(a). In a standard microscope, the CCD detection plane would be positioned at the exit port of the microscope, i.e at the optical plane F_{TL} conjugated with the objective focal plane F_{MO}. The image of a sample-object kept at a distance z_1 from F_{MO} would form on an optical plane, F_T, shifted by $D{=}M^2 z_1$ (M is the magnification of the microscope objective) in respect to the plane F_{TL}, therefore inside the microscope. In our configuration, we transfer the image out of the microscope by using an external telescope T inserted between the exit port of the microscope and the CCD. The telescope is positioned with its first focal plane in coincidence with the position of F_T, and its second focal plane in coincidence with the CCD detection plane. The telescope and the CCD are mounted on a translation stage that allows us to select different imaging planes by a rigid adjustment, $D{=}M^2 z$, of the component (T+CCD), D=0 being the position in which the first focal plane of the telescope coincides with F_{TL}.

Trapping beam path

As illustrated in Figure 1(a), the SLM is represented by a reflective thin lens and the microscope objective, MO, by its principal planes. The laser beam is reflected and modulated by the SLM in an array of spot focused on the plane F_{SLM}. This plane is imaged by the

microscope objective at a distance z from its focal plane F_{MO}. By applying the conjugation equation written in focal coordinates for the MO, we have:

$$zz^* = -f_{MO}^2 \tag{2}$$

where:

$$z^* = f_{SLM} + f_{MO} - d. \tag{3}$$

and d indicates the distance from the SLM to the first principal plane of the MO. Introducing Equation 2 in Equation 3, we obtain the expression for the trapping plane position, z, as a function of the other parameters, $z = z(f_{MO}, f_{SLM}, d)$:

$$z = -\frac{f_{MO}^2}{f_{SLM} + f_{MO} - d} \tag{4}$$

from which we easily derive Equation 1 in the Results.

The values for d and f_{MO} have been obtained by fitting the experimental curve shown in Figure 1(b). To obtain the curve, we calculated and displayed on the SLM phase DOEs with different focal lengths, f_{SLM}, and we optimized with an accuracy of 10nm the objective position, z_{ob}, which maximizes the intensity of the reflected signal produced by focusing the traps on the coverslip. In this condition, z_0=0 and the values of z_{ob} correspond to the values of z. From the fitting of the curve, we derived the following values: d= 833 mm and f_{MO}=1.5 mm.

Cell culture and beads preparation

Cell nuclei have been visualized using histone H2B tagged with GFP (generous gift from T. Kanda; The Salk Institute, La Jolla, CA). HeLa cells have been cultured on glass coverslips in Dulbecco's Modified Eagle Medium (Invitrogen, Cergy Pontoise, France), supplemented with fetal calf serum (10%), at 37^0C in a 5% CO_2 atmosphere. The cells have been transfected with the plasmid encoding H2B-GFP using FuGENE^{TM} 6 Transfection Reagent (Roche Molecular Biochemicals, Meylan, France), according to the manufacturer's instructions. The coverslips have been mounted in a thermostated open chamber, allowing for long time observation. The experiments have been performed at 37^0C in a 5% CO_2 atmosphere.

We used silica beads 2 μm in size (Bangs Laboratory Inc.). For the experiment with living cells, the beads were coated with RGD peptide according to the manufacturers procedure (Telios Pharmaceuticals Inc., CA USA).

FIG. 1: (a) Schematic of the imaging (green) and the trapping (red) beam paths. L - laser, SLM - spatial light modulator, DM - infrared dichroic mirror, MO - microscope objective, TL - tube lens, T - telescope; (b) Calibration curve for the measurement of d and f_{MO}.(c) Transmission image of a 3D structure of beads trapped in three planes at an axial distance of 2 μm. The imaging plane is adjusted at z_1=9.6μm, so that the intermediate plane of the structure results in focus.

FIG. 2: Relative positions (not in scale) of the trapping, imaging and objective plane with respect to the coverslip and the objective focal plane during an axial scan.

FIG. 3: (a)-(f) Selected sequence from a 3D DIC axial scan with a step of 200nm of 6 beads trapped by the laser. The imaging plane position, z_{IP}, in respect to the coverslip and the trapping plane position, z, which compensate for the objective movements, are indicated in the figure. As a results of the compensation, the circle is kept at a fixed high, z_0= 4.6 μm, from the coverslip. White bar = 5 μm. For the whole optical sectioning see Supplementary movie 1.

FIG. 4: Sequence of (a) transmission and (b) fluorescence images (step of 1μm) acquired during an axial scan where a circle of 6 beads is positioned and held on the dorsal cortex of a HeLa cell. The beads are kept at a fixed position while the objective scans a range of 8.2 μm, at step of 200 nm. Fluorescence images have been de-convoluted as explained in the text. For the whole fluorescence sectioning see Supplementary movie 2

FIG. 5: (a)-(f) Selection of 6 cross sections, at step of 0.8 μm, of an optical sectioning of the 3D structure shown in Figure 1 (c). The positions, z_{IP}, of the image plane in respect to the coverslip are indicated in the figure. In the original scan images are taken form z_{IP}=12.6 μm to z_{IP}=7.4 μm a step of 200 nm. For the whole optical sectioning see Supplementary movie 3

We thank the *platform 'Imaging of Dynamical Processes in Cellular and Developmental Biology'* of the IJM for the de-convolution of the fluorescence images. We thank Morad Zahid and Eric Steward for helpful advices in the realization of the system. This work was supported by the CNRS by the ARC (Association pour la Reserche sur Cancer) and by the Italian Ministry of Research (MIUR), project "Optical Tweezers for Biophysical Applications" (n. RBAU0157P2).

[1] Paddock S.W., *Confocal laser scanning microscopy*, BioTechniques **27**:992 (1999).

[2] Piston D.W., *Imaging living cells and tissues by two-photon excitation microscopy*, Trends Cell Biol. **9**:66 (1999).

[3] Oheim M., Loerke D., Chow R.H., and Stuhmer W., *Evanescent-wave microscopy: a new tool to gain insight into the control of transmitter release*, Philos. Trans. R. Soc. Lond. B Biol. Sci. **354**:307 (1999).

[4] Wouters F.S., Verveer P.J., and Bastianes P.I., *Imaging biochemistry inside cells*, Trends Cell Biol. **11**:203 (2001).

[5] Tramier M., Sanvitto D., Emiliani V., Durieux C., and Coppey-Moisan M., *FRET and fluorescence lifetime imaging microscopy in: Live Cell Imaging: A laboratory Manual.*

[6] Grier D.G., *A revolution in optical manipulation*, Nature **424**:810 (2003).

[7] Ashkin A. and Dziedzic J.M., *Optical trapping and manipulation of viruses and bacteria*, Science **235**:1517 (1987).

[8] Ericsson M., Hanstorp D., Hagberg P., Enger J., and Nystrom T., *Sorting out bacteria with optical tweezers*, J. Bacteriol. **182**:5551 (2000).

[9] Ishijima A., Kojima H., Funatsu T., Tokunaga M., Higuchi H., Tanaka H., and Yanagida T., *Simultaneous observation of individual ATPase and mechanical events by a single myosin molecule during interaction with actin*, Cell **92**:161 (1998).

[10] Thoumine O., Kocian P., Kottelat A., and Meister J.J., *Short-Term binding of fibroblast to fibronectin: optical tweezers experiments and probabilistic analysis*, Eur. Biophys. J. **29**:398 (2000).

[11] Svoboda K. and Block S.M., *Force and velocity measured for single kinesin molecules*, Cell **77**:773 (1994).

[12] Molloy J.E., Burns J.E., Kendrick-Jones J., Tregear R.T., and White D.C., *Movement and force produced by a single myosin head*, Nature **378**:209 (1995).

[13] Choquet D., Felsenfeld, D.P., and Sheetz M.P., *Extracellular matrix rigidity causes strengthening of integrin-cytoskeleton linkages*, Cell **88**:39 (1997).

[14] Galbraith C.G., Yamada K.M., and Sheetz M.P., *The relationship between force and focal complex development*, J. Cell Biol. **159**:695 (2002).

[15] Del Pozo M.A., Kiosses W.B., Alderson N.B., Meller N., Hahn K.M., and Schwartz M.A., *Intergin regulate GTP-Rac localized effector interaction through dissociation of Rho-GDI*, Nat. Cell Biol. **4**:232 (2002).

[16] Lambert M., Choquet D., and Mege R.M., *Dynamics of ligand-induced, Rac1-dependent anchoring of cadherins to the actin cytoskeleton*, J. Cell Biol. **157** (3):469 (2002).

[17] Emiliani V., Sanvitto D., Durieux C., and Coppey-Moisan M., *Integrin-cytoskeleton interaction investigated by multi force multi trap optical tweezers*, submitted (2004).

[18] Lenormand G., Henon S., Richert A., Simeon J., and Gallet F., *Elasticity of the human red blood cell skeleton*, Biorheology **40**:247 (2003).

[19] Visscher K., Brakenhoff G., and Krol J.J., *Micromanipulation by multiple optical traps created by a single fast scanning trap integrated with the bilateral confocal scanning laser microscope*, Cytometry **14**:105 (1993).

[20] Emiliani V., Sanvitto D., Zahid M., Gerbal F., and Coppey-Miosan M., *Multi Force optical tweezers to generate gradients of force*, Opt. Express **12**:3906 (2004).

[21] Dufresne E., Spalding G.C., Dearing M.T., Sheets S.A., and Grier D.G., *Computer-generated holographic optical tweezer arrays*, Rev. Sci. Instrum. **72**:1810 (2001).

[22] Melville H., Milne, G.F., Spalding G.C., Sibbett W., Dholakia K., and McGloin D., *Optical trapping of three-dimensional structures using dynamic holograms*, Opt. Express **11**:3562 (2003).

[23] Sinclair G., Jordan P., Courtial J., Padgett M., and Laczik Z.J., *Assembly of 3 dimensional structures using programmable holographic optical tweezers*, Opt. Express **12**:5475 (2004).

[24] Cojoc D., Emiliani V., Ferrari E., Malureanu R., Cabrini S., Proietti R.Z., and Di Fabrizio E., *Multiple optical trapping by means of diffractive optical elements*, Jap. Journal of Appl. Phys. **43**:3910 (2004).

[25] Gahagan K.T. and Swartzlander Jr G.A., *Optical vortex trapping of particles*, Optics Lett. **21**:827 (1996).

[26] Curtis J.E., Koss B.A., and Grier D., *Dynamic holographic optical tweezers*, Opt. commun. **207**:169 (2002).

[27] Lang M.J., Fordyce P.M., Engh A.M., Neuman K.C., and Block S.M., *Simultaneous, coincident optical trapping and single-molecule fluorescence*, Nat. Meth. **2**:133 (2004).

[28] Goksor M., Enger J., and Hanstrop D., *Optical manipulation in combination of single-cell*

studies, Appl. Optics **43**:4831 (2004).

[29] Hoffmann A., Meyer zu Horste G., Pilarczyk G., Monajembashi S., Uhl V., and Greulich K.O., *Optical tweezers for confocal microscopy*, Appl. Phys. B **71**:747 (2000).

[30] Di Fabrizio E., Cojoc D., Cabrini S., Kaulich B., Susini J., Facci P., and Wilhein T., *Diffractive optical elements for differential interference contrast X-ray microscopy*, Opt. Express **11**:2278 (2003).

[31] Geiger B., Bershadsky A., Pankov R., and Ymada K.M., *Transmembrane extracellular matrix-cytoskeleton crosstalk*, Nat. Rev. Mol. Cell Biol. **2**:793 (2001).

[32] Di Fabrizio E., Cojoc D., Emiliani V., Cabrini S., Coppey-Moisan M., Ferrari E., Garbin V., and Altissimo M., *Microscopy of biological sample through advanced diffractive optics from visible to X-Ray wavelength regime*, Microscopy research and technique (to be pulished 2005).

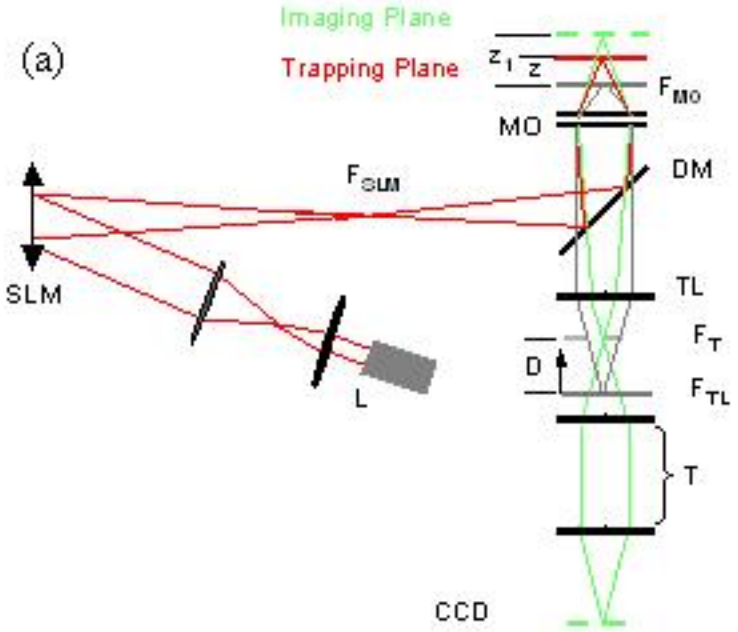

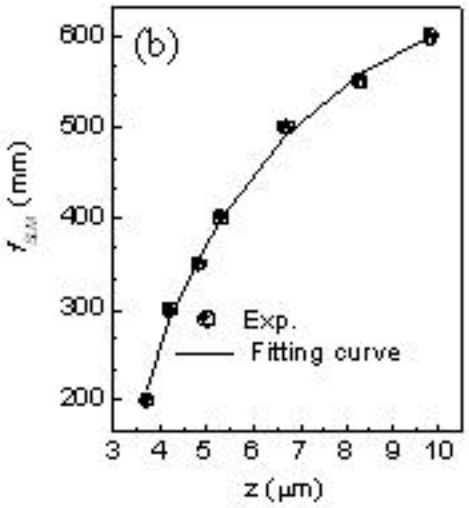

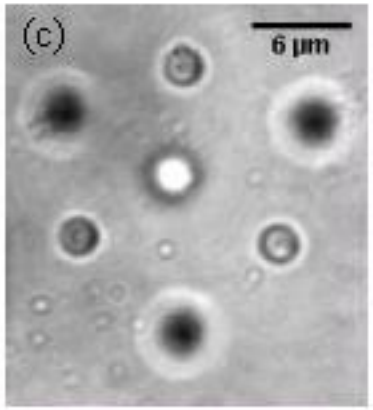

Emiliani et al. **Fig.1**

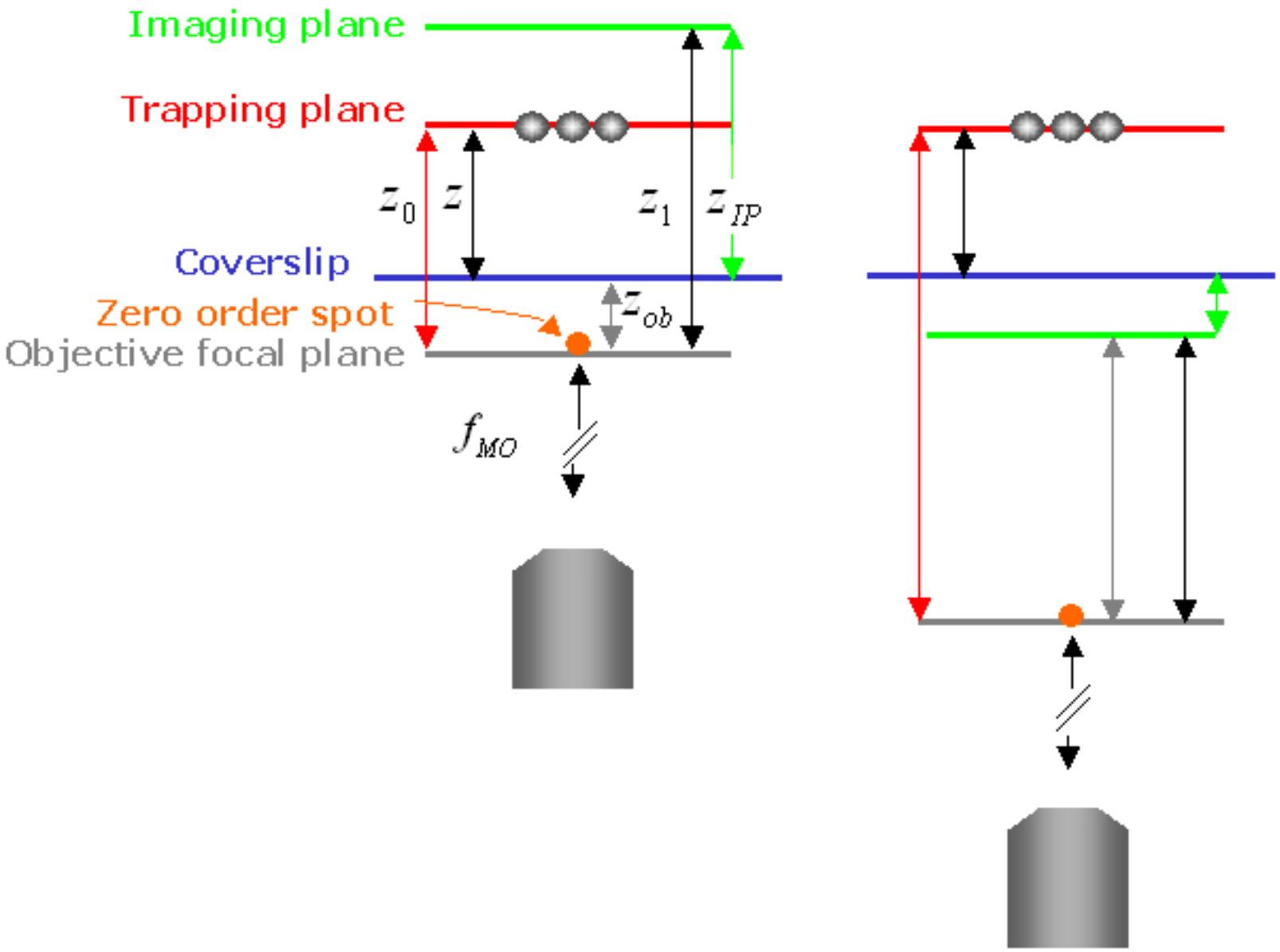

Emiliani et al. Fig.2

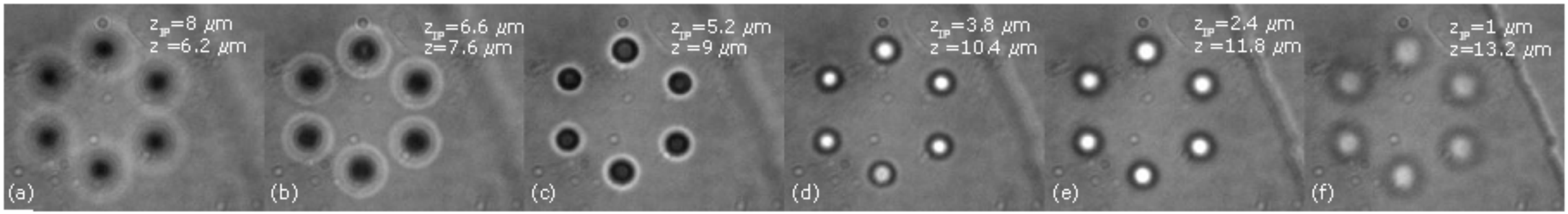

Emiliani et al. **Fig.3**

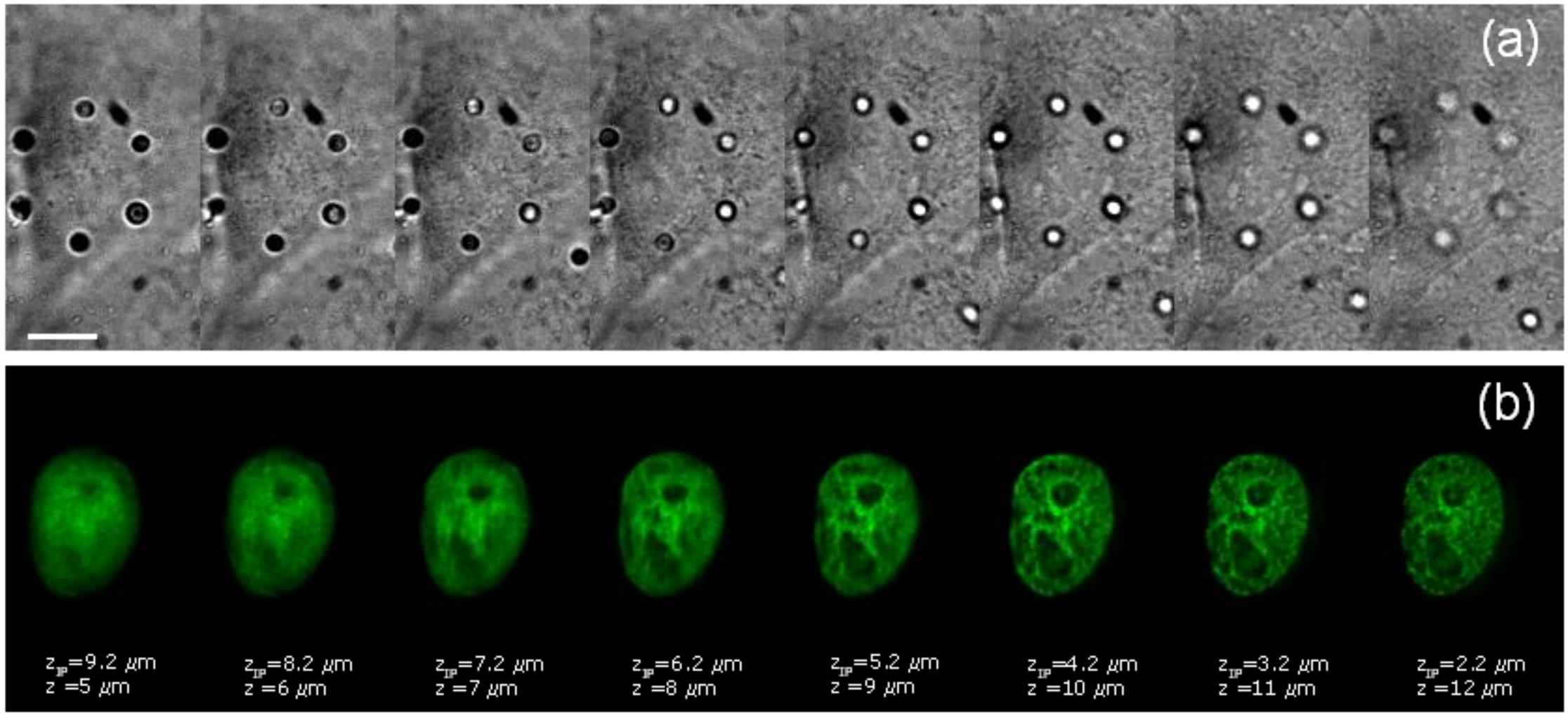

Emiliani et al. **Fig.4**

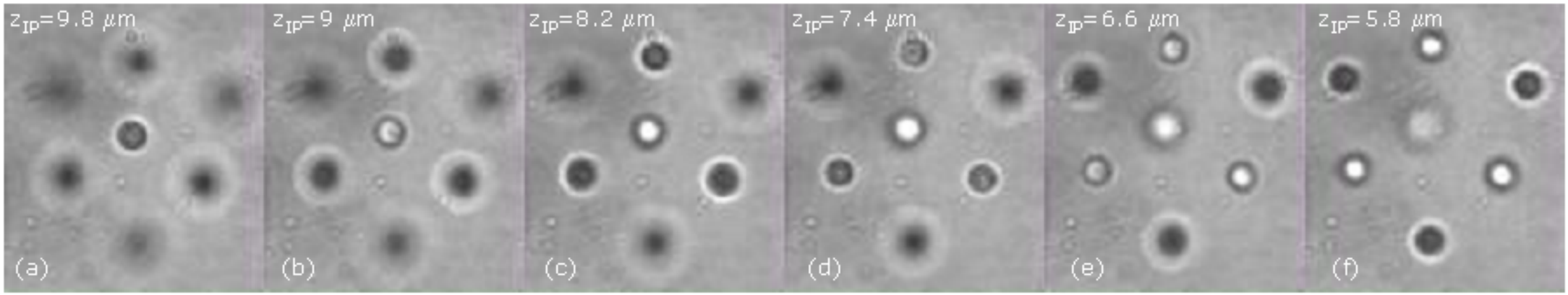

Emiliani et al. **Fig.5**